

RESONANT CHARACTERISTICS OF FREQUENCY SELECTIVE SURFACES ON FERRITE SUBSTRATES

J. C. Zhang and Y. Z. Yin

National Laboratory of Antennas and Microwave Technology
Xidian University
Xi'an, Shaanxi 710071, China

R. P. Yi

East China Research Institute of Electronic Engineering
Hefei 230031, China

Abstract—The resonant characteristics of frequency selective surfaces (FSSs) on in-plane biased ferrite substrates for the TE polarization are described. An approximate formula for evaluating the resonant frequency is presented. The tunable property of the resonant frequency of a dipole FSS is firstly demonstrated by the results obtained from the moment method (MM) and the waveguide simulator measurement. Then the approximate formula is validated by the MM as well as measured results already published in a previous paper. It is interesting to note that two separate resonances occur at any magnetic bias field, and both increase as the magnetic bias field increases. The fractional tuning range is investigated based on the approximate formula. The results show that it increases as the saturation magnetization increases and decreases as the center frequency increases.

1. INTRODUCTION

Frequency selective surfaces are widely used as filters and absorbers in microwave, millimeter wave and far infrared community [1–15]. They basically consist of periodic arrays of conducting patches or apertures on a conducting sheet. They exhibit total reflection or transmission in the neighborhood of the element resonance. Ferrite materials have a permeability tensor whose elements can be easily controlled through the use of a DC magnetic bias field. The extra degree of freedom

Corresponding author: J. C. Zhang (zhang00jch@yahoo.com.cn).

offered by the biased ferrite substrates can be used to obtain a number of novel characteristics. FSSs on ferrite substrates are well investigated for their tunable property [4–6]. In [5], a cross dipole FSS on a ferrite substrate is studied and a tuning range from 17.2 GHz to 19.2 GHz is obtained. In [6], the resonant characteristics of square loop FSSs on biased ferrite substrates are discussed based on the experiment results measured in a waveguide simulator.

For tunable FSSs [4–6, 9, 11], the resonant frequency and the tuning range are two important parameters. They can be accurately obtained from the full-wave MM. However, the MM is computationally intensive. In this paper, approximate formulas for evaluating the resonant frequency and the fractional tuning range are developed. Compared with the MM, the approximate formulas, which are simple algebraic expressions, have the advantage of fast computation, and they give us the algebraic relations between the resonant frequency along with tuning range and the saturation magnetization along with magnetic bias field. The tunable property of the resonant frequency of a dipole FSS on an in-plane biased ferrite substrate placed in a WR90 waveguide simulator is examined. Good agreement between the results obtained from the MM and the measured ones is observed. Then, an infinite planar FSS is investigated by the MM and the approximate formula. Again, good agreement is observed. A study on a square loop FSS presented in [6] suggests that the resonant frequencies calculated by the approximate formula agree well with the measured ones in [6]. Finally, a parametric study of the fractal tuning range is done based on the approximate formula.

2. THEORY

2.1. Analysis of FSSs on Ferrite Substrates by Moment Method

The analysis is carried out in the spectral domain. The electric field integral equation (EFIE) is applied; and for a FSS with isotropic media it can be written as [1]

$$\begin{cases} E_x^i = \frac{1}{T_x T_y} \sum_{m,n=-\infty}^{+\infty} \left(\tilde{G}_{xx} \tilde{J}_x + \tilde{G}_{xy} \tilde{J}_y \right) e^{-j(\alpha_m x + \beta_n y)} \\ E_y^i = \frac{1}{T_x T_y} \sum_{m,n=-\infty}^{+\infty} \left(\tilde{G}_{yx} \tilde{J}_x + \tilde{G}_{yy} \tilde{J}_y \right) e^{-j(\alpha_m x + \beta_n y)} \end{cases} \quad (1)$$

where the symbol ‘ \sim ’ denotes the Fourier transformation. \tilde{G}_{xx} , \tilde{G}_{xy} , \tilde{G}_{yx} , \tilde{G}_{yy} are transverse components of the spectral dyadic Green’s function. E_x^i , E_y^i are the incident fields due to the incident wave in the absence of the metallic layer. \tilde{J}_x , \tilde{J}_y are the electric currents induced on the metallic layer. T_x , T_y are the periodicities, and

$$\alpha_m = \frac{2\pi m}{T_x} + k_0 \sin \theta \cos \varphi$$

$$\beta_n = \frac{2\pi n}{T_y} + k_0 \sin \theta \cos \varphi$$

where k_0 is the wave number of free space, and θ, φ are the elevation and azimuth angles of incidence, respectively.

The main difference of the spectral domain analysis of FSSs with isotropic media and anisotropic media lies in different Green’s functions. The spectral Green’s function for ferrite FSSs is calculated by the recursive transformation method presented by Yang in [7]. The EFIE is solved by the Galekin’s MM. The rooftop basis functions are used to expand electric current [16]. After the electric current is solved, the scattering parameters are ready to be known.

2.2. Approximate Formula

In this section, an approximate formula for evaluating the resonant frequencies of FSSs on in-plane biased ferrite substrates for the TE polarization is established.

For a FSS embedded in an in-plane biased ferrite material which fills the entire space, the resonant frequency is given as

$$f = \frac{f_0}{\sqrt{\varepsilon_r \mu_r}} \quad (2)$$

In practice, the FSS is always with substrates of finite thickness. Then, (2) should be modified as

$$f = \frac{f_0}{\sqrt{\varepsilon_e \mu_e}} = \frac{f_d}{\sqrt{\mu_e}} \quad (3)$$

where ε_e , μ_e are the effective permittivity and permeability, respectively. And f_d is the resonant frequency when $\mu_e = 1$ (i.e., dielectrics). If the ferrite is unbiased, it can be considered as a dielectric material. Therefore, f_d is also the resonant frequency of the FSS on an unbiased ferrite substrate, called unbiased resonant frequency.

If the electric field of a TE incident wave is parallel to the bias direction, μ_r in (2) can be given as [8]

$$\mu_r = \frac{\mu^2 - \kappa^2}{\mu} \quad (4)$$

where

$$\mu = 1 + \frac{\gamma^2 H_0 4\pi M_s}{\gamma^2 H_0^2 - f^2}, \quad \kappa = \frac{f \gamma H_0 4\pi M_s}{\gamma^2 H_0^2 - f^2} \quad (5)$$

where $\gamma = 2.8 \text{ MHz/Oe}$, and H_0 , $4\pi M_s$ are the magnetic bias field and the saturation magnetization, respectively. It is assumed that the ferrite is saturated. μ_e can be approximately obtained from (4) by making $4\pi M_s$ half of the original value.

After some algebraic manipulations of (3)–(5), we can obtain

$$f^4 - (A + B)f^2 + AC = 0 \quad (6)$$

where $A = f_d^2$, $B = \gamma^2(H_0 + 4\pi M'_s)^2$, $C = \gamma^2 H_0(H_0 + 4\pi M'_s)$, and $4\pi M'_s = 4\pi M_s/2$.

(6) has two positive roots, which are written as

$$f_{1,2} = \sqrt{\frac{(A + B) \pm \sqrt{(A + B)^2 - 4AC}}{2}} \quad (7)$$

The two roots represent two resonant frequencies.

It is noted that the approximate formula is based on the unbiased resonant frequency. It is proposed to investigate the relations between the resonant frequency and the saturation magnetization as well as the magnetic bias field of the ferrite substrate. The influences of all other parameters, such as geometry of the element, periodicities, the thickness and dielectric constant of the substrate, and angle of incidence, are included in the unbiased resonant frequency.

3. NUMRICAL RESULTS

A dipole FSS prototype, as shown in Fig. 1, is fabricated and measured in a WR90 waveguide simulator [17], which contains two elements. Conducting patches are attached on the ferrite substrate. The parameters are: $\varepsilon_r = 12.8$, $4\pi M_s = 650 \text{ G}$, $d = 4.5 \text{ mm}$; $T_x = 11.43 \text{ mm}$, $T_y = 10.16 \text{ mm}$, $l = 8.1 \text{ mm}$, $w = 4.2 \text{ mm}$. d is the thickness of the substrate. Permanent magnets are used to bias the ferrite along the y -axis.

It is well known that the TE_{10} mode in a rectangular waveguide can be decomposed into two plane waves with incident angles

$$\theta = \arcsin \lambda/2a \quad (8)$$

and $\varphi = 0, \pi$, respectively. Where λ is the dielectric wavelength and a is the broader side of the rectangular. It is noted that the frequency responses of the FSS due to the two incident plane waves are not the same because of the anisotropic property of the ferrite.

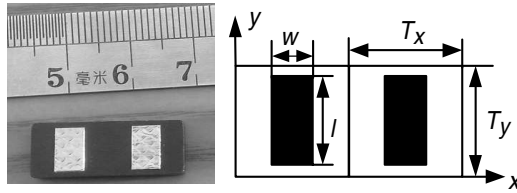


Figure 1. A patch FSS on a ferrite substrate and its dimensions.

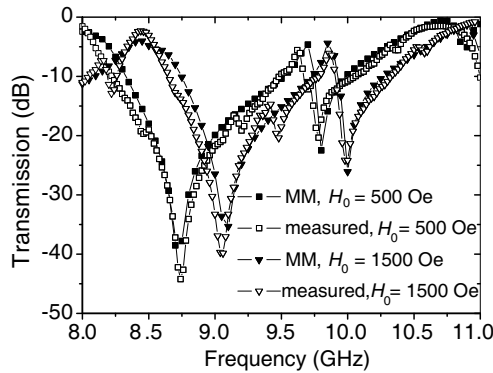


Figure 2. The transmission of the FSS shown in Fig. 1.

Figure 2 shows the transmission coefficients of the FSS versus frequency; both the MM and measured values are given for comparison. The results are in good agreement. It can be seen that the resonant frequency f_r increases from 8.70 GHz to 9.10 GHz as the magnetic bias field H_0 increases from 500 Oe to 1500 Oe.

Figure 3 shows the transmission of an infinite planar dipole FSS in a wide frequency band. The parameters are: $\epsilon_r = 13.5$, $4\pi M_s = 650$ G, $d = 0.5$ mm; $T_x = T_y = 10$ mm, $l = 8$ mm, $w = 1$ mm, $\theta = \varphi = 0.1^\circ$, TE polarized. The results are obtained from the MM. It is interesting

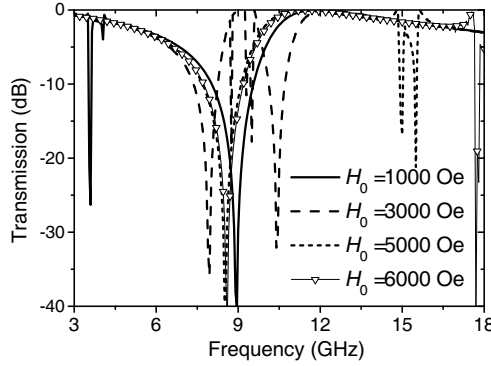


Figure 3. Transmission of an infinite planar dipole FSS on a ferrite substrate.

that the resonant frequency does not always increase as H_0 increases. For example, the resonant frequency is 8.95 GHz at $H_0 = 1000$ Oe, larger than 8.50 GHz at $H_0 = 5000$ Oe. The approximate formula will give a good interpretation for this characteristic.

Figure 4 shows the resonant frequency calculated by (7) versus the magnetic bias field H_0 . The MM results are also given for verification. Good agreement is demonstrated except some minor variations, which may be due to the errors from the approximation of μ_e . It is observed that there exist two resonances at any H_0 : one is smaller than f_d (8.80 GHz, obtained by MM), and the other larger. Both of them increase steadily as H_0 increases. The smaller one starts from zero and has a maximum of f_d , while the larger one starts from f_d and goes to infinity. In fact, for the larger resonant frequency, the curve has an asymptote of

$$f = \gamma (H_0 + 4\pi M'_s) \quad (9)$$

Now return to Fig. 3, the resonance $f_r = 8.95$ GHz at $H_0 = 1000$ Oe is the larger resonance, and it increases to 10.05 GHz, 15.45 GHz, 18.25 GHz at $H_0 = 3000$ Oe, 5000 Oe, 6000 Oe, respectively. While the resonance $f_r = 8.5$ GHz at $H_0 = 5000$ Oe is the smaller resonance. It can be seen that the smaller resonances at $H_0 = 5000$ Oe, 6000 Oe are almost the same. All these resonant characteristics are well demonstrated in Fig. 4. It should be noted that besides the two resonances there are other transmission minima that need further investigation.

Another interesting result observed from Fig. 3 is that as the resonance goes far away from f_d , it becomes irregular: tends to

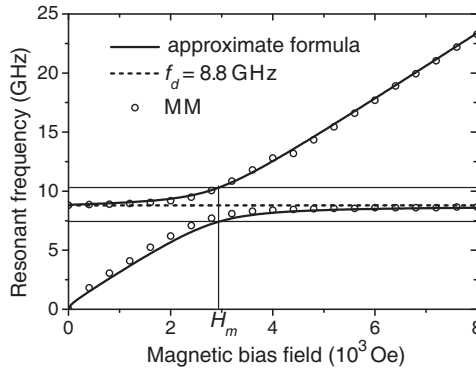


Figure 4. The resonant frequency of a dipole FSS on a biased ferrite substrate.

oscillate, or the bandwidth becomes extremely narrow. Besides, to avoid grating lobes the frequency should be less than $c_0/D/(1 + \sin \theta)$ for a square lattice, where c_0 , D are the light speed in free space and the periodicity, respectively. Therefore, only the resonances near f_d are appropriate for use. For convenience, only the one nearer f_d of the two resonances is considered. This can be clearly seen from Fig. 4: only the resonances between the two parallel lines, which have the same distance from the line of f_d , are considered. Under this assumption, the fractional tuning range is defined as

$$\delta = \frac{2(f_1(H_m) - f_d)}{f_d} \quad (10)$$

where H_m is the root of equation: $f_1 - f_d = f_d - f_2$ on H_0 .

For example, as shown in Fig. 4, when $H_0 = H_m = 2900$ Oe, the resonant frequencies obtained from (7) are $f_1 = 10.24$ GHz, $f_2 = 7.36$ GHz, respectively. And $f_1 - f_d = f_d - f_2 = 10.24 - 8.8 = 8.8 - 7.36 = 1.44$. Therefore, the fractional tuning range is $2.88/8.8 = 32.7\%$.

Note that the tuning range is not continuous, and there is a small gap between the smaller and the larger resonances because f_2 can not reach f_d until H_0 is infinitely large. Nevertheless, the fractional tuning range defined by (10) will give significant information.

Figure 5 shows the resonant frequencies of a square loop FSS presented in [6]. The unbiased resonant frequency f_d can be read from the figure at the point of zero magnetic bias field, which is about 11.6 GHz. Although the angle of incidence varies with frequency, the results obtained from the approximate formula are in good agreement

with the measured ones presented in [6]. Note that in [6] the frequencies below 7.5 GHz and above 15 GHz are not given.

Figure 6 shows the fractional tuning range versus $4\pi M_s$ at different f_d . The results show that the fractional tuning range increases as $4\pi M_s$ increases, and decreases as f_d increases. It is clear that the slope increases as f_d decreases. Therefore, great fractional tuning range is easier to be achieved for small f_d and large saturation magnetization cases.

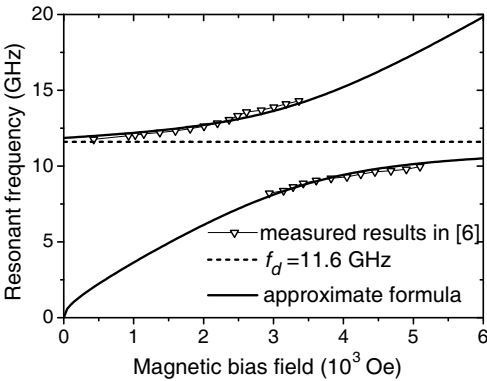


Figure 5. Resonant frequencies of a square loop FSS in a waveguide simulator.

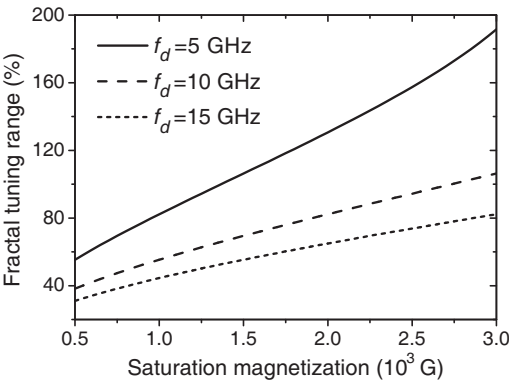


Figure 6. Fractional tuning range of FSSs on a biased ferrite substrate.

4. CONCLUSION

The resonant characteristics of FSSs on in-plane biased ferrite substrates for the TE polarization are carefully investigated. An approximate formula is developed for evaluating the resonant frequencies. Waveguide simulator measurement of a dipole FSS on a ferrite substrate is done. The MM results are in good agreement with the measured. The approximate formula results are validated by means of MM results and measurement results from the open literature. Two resonances occur at any magnetic bias field: one is smaller than the unbiased resonant frequency, and the other larger. Both resonant frequencies increase as the magnetic bias field increases. The fractional tuning range is discussed based on the approximate formula. The center frequency of the tuning range is the unbiased resonant frequency. The fractional tuning range steadily increases as saturation magnetization increases, and decreases as center frequency increases.

REFERENCES

1. Vacchione, J. D., "Techniques for analysing planar, periodic, frequency selective surface systems," Ph.D. Thesis, University of Illinois at Urbana-Champaign, 1990.
2. Luo, G. O., W. Hong, Q. H. Lai, et al., "Frequency-selective surfaces with two sharp sidebands realised by cascading and shunting substrate integrated waveguide cavities," *IET Microw. Antennas Propag.*, Vol. 2, 23–27, 2008.
3. Mudar, A.-J. and N. Behdad, "A new technique for design of low-profile, second-order, bandpass frequency selective surfaces," *IEEE Trans. Antennas Propagat.*, Vol. 57, 452–459, 2009.
4. Cheng, L. Y., "Analysis of frequency selective surfaces with ferrite substrates," Ph.D. Dissertation, Dept. Elect. Eng., Univ. of Central Florida, 1996.
5. Li, G. Y., Y. C. Chan, T. S. Mok, and J. C. Vardaxoglou, "Analysis of frequency selective surfaces on a biased ferrite substrate," *Int. J. Electronics*, Vol. 78, 1159–1175, 1995.
6. Chang, T. K., R. J. Langley, and E. A. Parker, "Frequency selective surfaces on biased ferrite substrates," *Electronics Letters*, Vol. 30, 1193–1194, 1994.
7. Yang, H.-Y. D., "A spectral recursive transformation method for electromagnetic waves in generalized anisotropic layered media," *IEEE Trans. Antennas Propagat.*, Vol. 45, 520–526, 1997.

8. Pozar, D. M., *Microwave Engineering*, 3rd edition, Wiley-Interscience, New York, 2004.
9. Ma, D. and W. S. Zhang, "Mechanically tunable frequency selective surface with square-loop-slot elements," *Journal of Electromagnetic Waves and Applications*, Vol. 21, No. 15, 2267–2276, 2007.
10. Guo, C., H. Sun, and X. Lu, "A novel dualband frequency selective surface with periodic cell perturbation," *Progress In Electromagnetics Research B*, Vol. 9, 137–149, 2008.
11. Ucar, M. H. B., A. Sondas, and Y. E. Erdemli, "Switchable splitting frequency selective surfaces," *Progress In Electromagnetics Research B*, Vol. 6, 65–79, 2008.
12. Zhang, J. C., Y. Z. Yin, and J. P. Ma, "Frequency selective surfaces with fractal four legged elements," *Progress In Electromagnetics Research L*, Vol. 8, 1–8, 2009.
13. Oraizi, H. and M. Afsahi, "Design of metamaterial multilayer structures as frequency selective surfaces," *Progress In Electromagnetics Research C*, Vol. 6, 115–126, 2009.
14. Farahat, A. E. and K. F. A. Hussein, "Spatial filters for linearly polarized antennas using free standing frequency selective surface," *Progress In Electromagnetics Research M*, Vol. 2, 167–188, 2008.
15. Zhuang, W., Z. H. Fan, D. Z. Ding, and Y. Y. An, "Fast analysis and design of frequency selective surface using the GMRESR-FFT method," *Progress In Electromagnetics Research B*, Vol. 12, 63–80, 2009.
16. Glisson, A. W. and D. R. Wilton, "Simple and efficient numerical methods for problems of electromagnetic radiation and scattering from surfaces," *IEEE Trans. Antennas Propagat.*, Vol. 28, 593–603, 1980.
17. Hannan P. W. and M. A. Balfour, "Simulation of a phased array antenna in waveguide," *IEEE Trans. Antennas Propagat.*, Vol. 13, 342–252, 1965.